IEEE Access
Multidisciplinary | Rapid Review | Open Access Journal

Received January 19, 2020, accepted February 2, 2020, date of publication February 10, 2020, date of current version February 19, 2020.

Digital Object Identifier 10.1109/ACCESS.2020.2973035

Reliability Assessment of Coordinated Urban Transportation and Power Distribution Systems Considering the Impact of Charging Lots

CHI ZHANG[1], (Student Member, IEEE), XIA ZHAO[1], (Member, IEEE), MOHAMMAD SHAHIDEHPOUR[2], (Fellow, IEEE), WENYUAN LI[1], (Life Fellow, IEEE), LILI WEN[3], AND ZHIFANG YANG[1], (Member, IEEE)

[1]State Key Laboratory of Power Transmission Equipment & System Security and New Technology, Chongqing University, Chongqing 400044, China
[2]Electrical and Computer Engineering Department, Illinois Institute of Technology, Chicago, IL 60616, USA
[3]State Grid Chongqing Economic Research Institute, Chongqing 400015, China

Corresponding authors: Xia Zhao (zx@cqu.edu.cn) and Mohammad Shahidehpour (ms@iit.edu)

This work was supported in part by the National 111 Project of China.

ABSTRACT Owing to spatiotemporal flexibility of electrical vehicles (EVs), EVs will introduce new synergies between the urban traffic system (UTS) and power distribution system (PDS). As a mobile charging load, arranged EV charging can not only provide more flexibility for power system optimization, but also influence the traveling time and other mobility-related characteristics of EVs. However, there are few studies that consider the impact of the coupling facility (such as parking lot with charging facilities) on UTS reliability, as well as the reliability of UTS and PDS (referred to as PTS). Therefore, it is necessary to extend the original research scope to incorporate the traffic system simulation into the collaborative analysis of the coordinated PTS. This paper first develops a new simulation framework for the coordinated UTS and PDS coupled with commercial charging lots (CLs). Then, a new method is illustrated for measuring the reliability of a coordinated UTS and PDS. At last, a novel unified PTS reliability index considering both UTS and PDS reliability indices are presented.

INDEX TERMS Electric vehicles (EVs), power distribution system (PDS), urban traffic system (UTS), commercial charging lots (CLs), reliability assessment, simulation of urban mobility (SUMO).

NOMENCLATURE

A. INDICES AND SETS

N^T	Total branches in the urban traffic system
N^{CL}	Total number of charging spots in one CL
p, q	Index of nodes in urban traffic system
j	Index of vehicles
k	Index of charging spots in the CL
r	Index of PTS reliability assessment iteration
i	Index of substep in SUMO simulation
UTS	Urban traffic system
PDS	Power distribution system
PTS	Power and transportation system
CLs	Charging lots

B. PARAMETERS

SOC^{max}	Battery's upper charging limit
SOC^{min}	Battery's lower charging limit
η	Charging efficiency
P	Constant charging power of EVs
C^j	Capacity of j^{th} EV
C^P	Energy is not supplied cost of PDS
C^T	Travel time cost of UTS

C. VARIABLES

L_{pq}	Edge between nodes p and q
l_{pq}	Length of edge between nodes p and q
j_{pq}	Vehicle that has traveled L_{pq}
n_{pq}	Total number of vehicles that traveled L_{pq}
n_{pq}^{in}	Total *number of* vehicles that have entered L_{pq}
n_{pq}^{out}	Total number of vehicles that reside outside L_{pq}

The associate editor coordinating the review of this manuscript and approving it for publication was Ahmed F. Zobaa.

TT_{pq}^{free}	Free-flow travel time for L_{pq}
PTT_{pq}	Planning travel time for L_{pq}
BI_{pq}	Buffer travel time for L_{pq}
TTI_{pq}	Travel time index for L_{pq}
$TT_{pq}^{95\%}$	95th percentile travel time for L_{pq}
PTT_{pq}^{ave}	Average planning travel time for L_{pq}
BI_{pq}^{ave}	Average buffer travel time for l_{pq}
TTI_{pq}^{ave}	Average travel time index for L_{pq}
$TT_{pq}^{95\%,ave}$	Average 95 percentile travel time for L_{pq}
$\overline{TT}_{pq}$	Mean travel time for L_{pq}
VMT_{pq}	VMT for L_{pq}
t_j^{arr}	Time of arrival at CL for j^{th} vehicle
t_j^{dep}	Time of departure from CL for j^{th} vehicle
t_j	Time point for j^{th} vehicle charging at CL
SOC_j^{arr}	Initial SOC when j^{th} EV arrives at CL
SOC_j	SOC of j^{th} vehicle charging at CL

Other notations are defined in the text.

I. INTRODUCTION

With the continuous growth of the world population and the improvement of living standards in developing countries, the number of vehicles has been soaring all over the world. This phenomenon causes a great burden to the traffic congestion in commuting hours, as well as air pollution[1]. The deployment of electric vehicles (EVs) provides a unique opportunity to deal with these problems. At the same time, the rapid development of EVs will bring new challenges to the management of both the urban traffic systems (UTS) and the power system (PDS) [2].

Existing studies on the correlation between UTS and PDS are briefly reviewed. In terms of the power system, the spatiotemporal flexibility of EV charging has been considered in recent years. Arranged EV demand makes it possible to provide ancillary services with higher quality [3], regulation of voltage [4], load balancing [5] for system integrated with renewable energy resources, and maintain the peak power[6]. According to the historical vehicle data[7], most studies model the probability distribution of daily trip distance, arrive time, and initial SOC of EVs [8]. Reference [9] uses queuing theory to model the drivers at each charging facility and predict the average queuing time and possible waiting time. Moreover, some studies also use data to predict more explicit route for vehicles. GPS-enabled trajectory data is used to provide the recorded route of vehicles in [10]. Recently, some methods based on machine learning algorithm have been presented to model and predict the EVs traveling behavior. Reference [11] presents a new clustering-based short-term load forecasting method using the deep neural network to forecast the household and EV demand. Most studies use the modeled EV traveling behavior to evaluate the complicated interactions among different types of EVs and chargers [12], to solve the charging station ''overstay'' problem [13], to determine the location of public charging stations [10], and to optimize the operation cost of the power system considering different scenarios of EVs penetration [14].

In terms of the transportation system, it can leverage spatiotemporal flexibility of EV to optimize the stopping place for vehicles and manage traffic flow during afternoon commuting rush hours. EV drivers can reduce their charging costs by using optimal strategies based on the provided incentives from the power system operator [15]. Reference [16] considers the energy consumption in the area of travel prediction. Reference [17] proposes a collaborative algorithm with two non-profit entities, each representing one of the coupled networks in the market. The distribution of locational marginal pricing is recalculated and adapted continuously according to the users' trips and behavior in [18].

As described above, EVs will introduce new synergies between the UTS and PDS (referred to as power and transportation system, PTS). Interdependent power and transportation network operators can leverage the flexible nature of this energy demand [19] or combine the wireless communication technology to improve the reliability of the corresponding networks [20], [21]. Therefore, it is necessary to extend the original research scope to incorporate the traffic system simulation into the collaborative analysis of coordinated PTS.

However, few studies take the impact of the coupling facility on the reliability of the UTS or the coordinated PTS into consideration. Reliability indices of the power system are considered in [14], [22]. References [23] and [24] accept some driving-related factor to meet the requested quality of charging service. Based on the Wardrop user equilibrium (UE) that models the EV traffic flow [25], the static travel simulation is time-divided to approximate the realistic travel simulation under congestion [26]. Reliability studies of urban transportation and power distribution systems in the above references only consider the reliability of the power system or evaluate the reliability from the perspective of the EV charging service requirement. The reliability of UTS in the system level needs to be evaluated. What's more, the interaction of EVs with other traffic factors have not been taken into account [24]. Explicitly, the circumstance described in the original paper, such as the vehicles breaking on the road and the drivers changing original destination to another charging station, would force other vehicles (including EVs) to change the original routes. The changed routes of other vehicles have not been considered. What is more, the reliability indices evaluated in this paper are all indices referring to EVs. The impact of EVs on the integrated system has not been clarified.

From the general perspective, the commercial CLs can attract vehicles, including EVs, to park and charge. Consequently, the parking pattern not only influences traffic flow but also provides an additional option for improving the reliability of PDS. In terms of the UTS, the plan of commuters to park at a CL relieves congestion pressure on the traffic system during commuting rush hours because this option makes more room for other motor vehicles on the road [27]. In terms of the PDS, EVs charging at commercial CLs will

charge less at home. Compared with charging at home only, additional charging places, such as commercial CLs, decrease the charging demand at home.

However, the evaluation of the impact of CLs on the reliability of PTS is a complex problem. The reason is that the static path does not change with the time under traffic congestion [26]. Furthermore, the high randomness of EVs is derived from the variability of the traffic system operation condition, such as traffic accidents and real-time road management. EV mobility characteristics represent composite factors, such as the scenario-related road conditions, driver behaviors, as well as the traffic control strategies [28]. The impact of these composite factors is difficult to describe by mathematical formulations.

To deal with this problem, real traffic system simulation is an excellent selection, which not only provides the real-time EV charging load profile but also considers traffic conditions in a realistic situation. Simulation of Urban Mobility (SUMO) [28] is a popular microscopic road traffic simulator. SUMO is more precise than macroscopic models, especially when individual routes need to be simulated [29]. Not only the moving vehicles but also traffic lights, pedestrians, buses, and bicycles, are involved in SUMO microscopic simulation. Moreover, in SUMO, the movement of individual vehicles is simulated to be more consistent with real scenarios based on car-following [30] and lane-changing [31] theories. The element modeling mechanism of SUMO allows researchers to consider real traffic scenarios. Therefore, in order to evaluate our purposed problem, it is the right choice for us to use SUMO to do the UTS simulation.

The contributions of this paper are as follows:

1) *A new reliability assessment framework is built for the cooperated PTS with CLs.*
   Considering the function of CL in the UTS and PDS, we present a new framework to evaluate the impact of the CL on coordinated PTS reliability in system-level.
2) *A novel reliability evaluation method for cooperative PTS with CLs is presented.*
   Time-varying traffic flow under congestion is realized by SUMO to model more realistic scenarios in the traffic system. SUMO cooperating with MATLAB simulates the process of coordinated PTS reliability assessment during afternoon commuting rush hours.
3) *A new unified reliability index for coordinated PTS with CLs is proposed.*

The reliability indices of UTS and PDS in system-level are introduced to quantify the reliability of the integrated system.

The remainder of this paper is organized as follows: The framework and main implementation steps for this framework are organized in Section II. The interaction model between the UTS and PDS is first discussed in Section III, and then traffic system simulation by SUMO and reliability index analysis are discussed. The reliability estimation method of the power system is also presented in this section. A novel reliability assessment approach for a coordinated PTS is proposed. Numerical studies are demonstrated in Section IV, and conclusions are drawn in Section V.

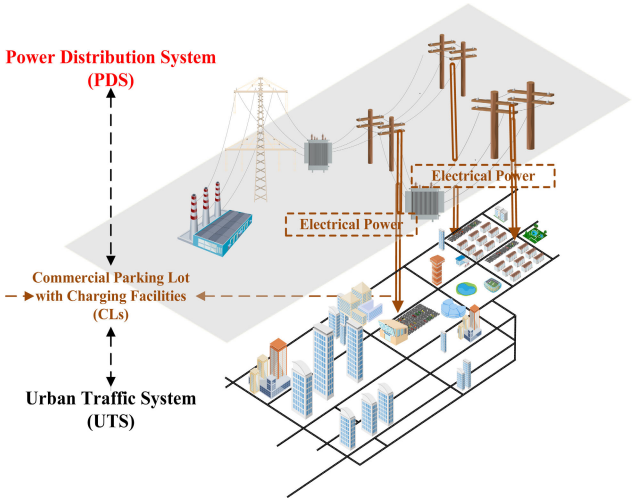

FIGURE 1. Proposed PTS framework with coordinated UTS and PDS.

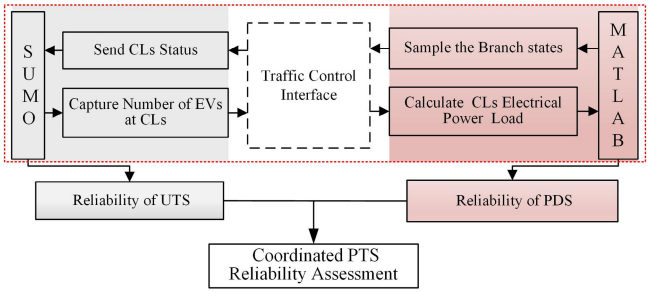

FIGURE 2. The interface between the UTS (SUMO) and PDS (MATLAB).

II. FRAMEWORK OF THE PROPOSED METHOD

A. FRAMEWORK OF COORDINATED PTS WITH CLS

In the proposed framework, the UTS and PDS, coupled EV charging lots, are referred to as a coordinated PTS. CLs play an essential role in improving the reliability of both systems; in particular, CLs located in commercial areas can give more benefits for PTS coordination. Therefore, in this paper, the UTS and PDS are coordinated through commercial area CLs. The reliability of the two systems is estimated first, and that of the coordinated PTS is considered accordingly. The cooperation of the integrated UTS and PDS is simulated in parallel by SUMO and MATLAB, and then, reliability indices that have been widely used for decades in both traffic and power systems are chosen to measure the performance of each system. Finally, a novel unified indicator, the reliability cost of the coordinated PTS (RCPTS), is proposed to quantify the performance of the coordinated PTS. In this paper, all CLs refer to CLs built-in commercial areas. Figure 1 shows a representation of the PTS coordination coupling a UTS and PDS with CLs.

B. OUTLINE OF THE PROPOSED FRAMEWORK REALIZATION

From the above, it can be indicated that the reliability of a PTS relies on the coordinated operation of the UTS and PDS.

However, the major difficulties in assessing the reliability process lie in the following two aspects: 1) the coordinated PTS operation needs to cooperate on a short-term scale between the UTS and PDS simulations and 2) a unified PTS reliability indicator that can comprehensively describe the coordinated systems needs to be developed.

As illustrated in figure 2, the proposed framework realization approach is constructed by the following 4 steps:

1) *UTS Simulation:* Use SUMO to generate each edge travel time index from the travel time captured on each edge and then obtain the averaged indices for each edge by considering the overall system information as the weight.
2) *PDS Simulation:* Use Monte Carlo simulation (MCS) to sample the working status of the branches for the PDS. MCS in MATLAB gives feedback to SUMO on the state of feeders that are interconnected by the CLs. Then, SUMO determines whether EVs can charge at a CL or not. The charging demand data are then provided as feedback to MATLAB from SUMO and added to the original bus load.
3) *Coordinated System Simulation:* The UTS and PDS are simulated simultaneously at specific intervals. MATLAB sends the working status of the charging facilities, and SUMO sends the real-time EV charging data to MATLAB at the same simulation interval. The bi-directional communication between SUMO and MATLAB occurs via a traffic control interface.

III. RELIABILITY ASSESSMENT OF THE COORDINATED PDS AND UTS

A. BI-DIRECTIONAL COMMUNICATION BETWEEN UTS AND PDS

In this paper, we propose an interactive simulation platform for evaluating the reliability of the coordinated PTS using MATLAB and SUMO. In this approach, the CLs are used as storage for traffic flow, including EVs, coupling the UTS and PDS. The CLs, with this function, will influence the travel time reliability and EV charging performance as well. In our work, a simulation process for the coordinated PTS reliability assessment is presented and illustrated in figure 3. The proposed process uses TraCI4MATLAB[32] which is a traffic control interface (TraCI) in MATLAB that realizes bidirectional communication, which allows the power system reliability assessment written in MATLAB to interact with SUMO.

We focus on the afternoon commuting rush hour (i.e., 16:00 - 21:00). The steps in the MCS begin at 16:00. SUMO and MATLAB will run in parallel until the one-loop simulation ends up at 21:00.

As shown in figure 3, the branch states are sampled at the beginning of each loop, and the topology of the PDS network is updated accordingly. MATLAB then checks whether there is load curtailment. Updated charging load data will be sent

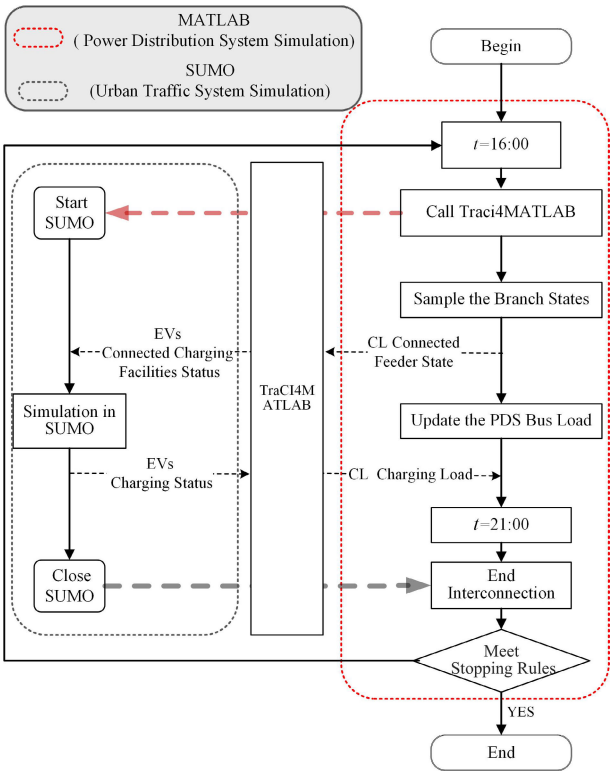

FIGURE 3. Reliability assessment of coordinated PTS.

as feedback as the SUMO simulation runs. Precisely, as soon as SUMO starts, in each simulation step, TraCI4MATLAB will extract the EV charging load, as well as other related and useful geographic information from SUMO, and send it to MATLAB. The EV charging load will be added to the original load of a bus to generate the updated bus load profile. In each loop, once there is an outage, whether to cut the load is checked. At the end of the whole simulation, calculate the expected energy not supplied (EENS).

During the coordinated PTS reliability analysis, TraCI4MATLAB extracts useful information from one system and sends it to another. Specifically, after the network branch states are sampled, TraCI4MATLAB extracts the working status of the charging facilities to SUMO. Then, SUMO sets the charging status of the parked EVs. The charging load amount is extracted from SUMO by TraCI4MATLAB to calculate the extra EV charging demand at the CLs. Regarded as an information interface, TraCI4MATLAB is used to translate the EV time-varying routing to the PDS time-varying charging load. Furthermore, as the EV charging strategy affects the EV charging demand for the PDS, TraCI4MATLAB also sends the EV charging strategies at the CLs to realize the EV coordinated charging strategy in SUMO.

The next loop, which represents the afternoon commuting rush hour of the next day, runs the same process of cooperation between the PDS MATLAB simulation and the UTS SUMO simulation. Because we aim to estimate the impact of CLs in commuting rush hours, we consider only

16:00 - 21:00 on weekdays. We repeat the same process until the PDS MCS meets the end criterion.

Next, the reliability assessments of the UTS and PDS are presented in parts B and C, respectively. The coordinated PTS assessment is proposed in part D. Finally, the simple coordinated charging strategy is briefly presented in part E.

B. TRAVEL TIME RELIABILITY OF UTS

Travel time reliability (TTR) measures the extent of an unexpected travel delay in traffic [33]. A reliable transportation system provides users with a consistent range of predict travel times [34]. Therefore, TTR is a critical performance indicator for a UTS. The most effective methods of measuring TTR are the 95th percentile travel time ($TT^{95\%}$), travel time index (TTI), buffer index (BI), and planning time index (PTI). $TT^{95\%}$ estimates delays on specific routes during the most massive traffic days. The TTI is a measure of how long, on average, travel times will be during congestion hours. The BI represents the additional time travelers must add to their average travel time to ensure on-time arrival. The PTI represents the total time a traveler should allow to ensure on-time arrival. The $TT^{95\%c}$, the TTI, the PTI, and the BI are all used to quantify the degree of late time arrivals.

In order to estimate the impact of CLs on UTS travel time reliability, the edge-based indices calculated from the metadata captured on edges are presented first, and then, average edge indices are used to reflect the TTR performance of the traffic system. The $TT_{pq}^{95\%}$ can be obtained from the collected data directly, and the other three indices [34] are,

$$TTI_{pq} = \frac{\sum_{j=1}^{n_{pq}} TT_{pq,j}}{n_{pq}} \tag{1}$$

$$PTI_{pq} = \frac{TT_{pq}^{95\%}}{T_{pq}^{free}} \tag{2}$$

$$BI_{pq} = \frac{TT_{pq}^{95\%} - \overline{TT_{pq}}}{T_{pq}^{free}} \times 100\% \tag{3}$$

where $TT_{pq,j}$ is the travel time of the j^{th} vehicle on L_{pq} and $\overline{TT}_{pq}$ is the mean travel time from the vehicle travel time data on L_{pq}.

For L_{pq}, T_{pq}^{free} is the time that one vehicle spends traveling on L_{pq} at the free-flow speed. We assume that the maximum speed for each vehicle in the UTS is 30 miles per hour and that 60% of the maximum speed is the free-flow speed. Thus, the travel time of one vehicle at the free-flow speed on L_{pq} is TT_{pq}^{free}. In contrast to the other indices, the BI is expressed as a percentage.

Accordingly, the indices calculated above only quantify network-partial time-consumer attributes, while the network-wide average indices estimate the weighted average UTS reliability performance, especially considering the interactions and correlations among all edges. Therefore, these weighted indices are more useful for analyzing the impact of commercial CLs on the UTS.

Here, the vehicle miles traveled (VMT)[35], [36] on each edge is accepted as the weight of each edge. The VMT is calculated as the sum of miles traveled by each vehicle. For one vehicle, the VMT on one specific edge is the length of that edge. In one specific period, many vehicles will travel across this edge. Therefore, for one edge, the VMT, calculated by multiplying the corresponding number of vehicles with the edge length, is the weighting factor used to calculate the edge-averaged TTR indices as follows,

$$VMT_{pq} = l_{pq} \sum_{j_{pq}=1}^{n_{pq}^{veh}} t_{pq,j} \tag{4}$$

In this paper, we calculate VMT_{pq} by using SUMO simulation results[37], where the SUMO simulation-based VMT_{pq} is expressed as,

$$VMT_{pq} = (n_{pq}^{in} + n_{pq}^{out}) \times l_{pq} \tag{5}$$

Then, the network-wide weighted edge-averaged indices TTI, PTI, and BI are,

$$TT_{pq}^{95\%,\text{ave}} = \frac{TT_{pq}^{95\%} \times VMT_{pq}}{\sum_{l_{pq}=1}^{N^T} (VMT_{pq})} \tag{6}$$

$$TTI_{pq}^{\text{ave}} = \frac{TTI_{pq} \times VMT_{pq}}{\sum_{l_{pq}=1}^{N^T} (VMT_{pq})} \tag{7}$$

$$PTI_{pq}^{\text{ave}} = \frac{PTI_{pq} \times VMT_{pq}}{\sum_{l_{pq}=1}^{N^T} (VMT_{pq})} \tag{8}$$

$$BI_{pq}^{\text{ave}} = \frac{BI_{pq} \times VMT_{pq}}{\sum_{l_{pq}=1}^{N^T} (VMT_{pq})} \tag{9}$$

figure 4 shows the simulation process to assess the UTS reliability when vehicles, including EVs, plan to stop and charge at CLs.

1) *Build the SUMO Simulation Data:* Specified scenarios are built using traffic flow data (e.g., OD matrix) [38] for the UTS. More detailed information is provided in Section IV.
2) *Data Collection for SUMO:* Traffic flow data, such as vehicle speed and vehicle location, are captured by SUMO edge sensors during the simulation. Each edge is equipped with point-based sensors to capture the traffic data to estimate travel times and TTR.
3) *Calculate Reliability Indices:* After simulation in SUMO, (1), (2), and (3) are used to calculate the reliability indices based on travel times on edges and then calculate the edge-averaged indices. We focus on TTR in the afternoon commuting rush hour (16:00-21:00), and individual traffic data are used to calculate the related travel time.

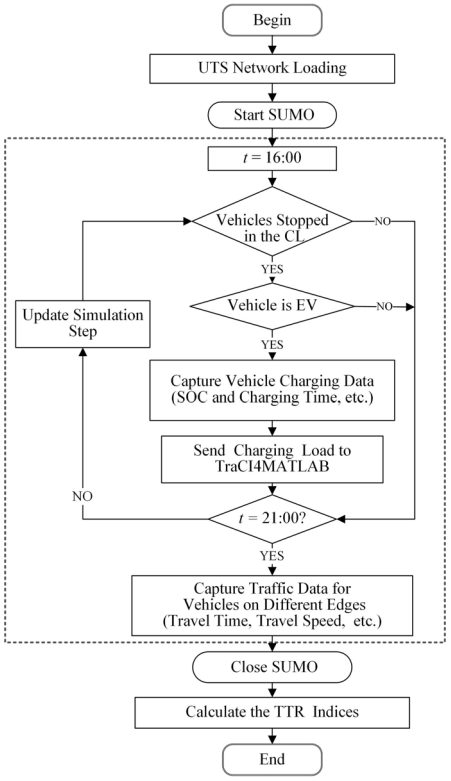

FIGURE 4. Travel time reliability assessment of UTS.

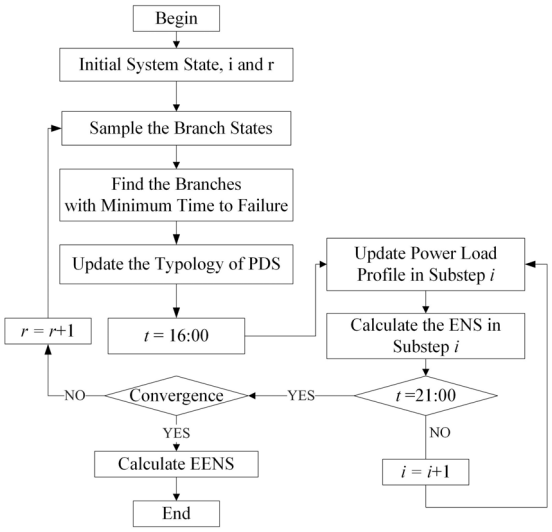

FIGURE 5. Power distribution system reliability assessment.

C. DRELIABILITY OF PDS

MCS is applied in this paper to sample the PDS topology status and is presented in figure 5 [39]. The procedure for sampling the system state is illustrated in the following steps,

1) Obtain the reliability data, such as the failure rate and failure duration for each component;
2) Specify the initial state. The simulation starts from the normal system state in which all components are in work status;
3) Assume the times to failure for all branches are all have an exponential distribution [39], [40]. Generate random numbers [0–1] for each component and determine its time to failure (TTF) according to the failure distribution of each element.
4) Find the branch with the minimum TTF [40];
5) Select this branch as the failed component. Because the study period is short in this paper, which is just the length of the afternoon commuting rush hours, we assume that the failed component could not be repaired during these hours;
6) Update the varying EV charging load in each substep i, and add it to the original bus load data;
7) Evaluate the energy not supplied (ENS) in each substep. If there is no branch out of work, the ENS is set to zero;
8) Check whether the MCS achieves convergence. If it does not meet the simulation ending rules, proceed to Step 3); otherwise, the simulation process is terminated, and proceed to Step 9);
9) Calculate the reliability indices, expected energy not supplied (EENS) [39],

$$EENS = \frac{\sum_{r=1}^{N_r} \sum_{i=1}^{N_i} ENS}{N_r \times N_i} \tag{10}$$

where N_i is the number of substeps in each iteration and N_r is the number of iterations during the simulation.

D. COORDINATED PTS RELIABILITY ASSESSMENT

After completing the simulations, we assess the reliability of the coordinated PTS. In a real scenario, EVs can choose to park at any location and time. Therefore, we adjust the PDS reliability index accordingly. To obtain a unified indicator for the coordinated PTS, we present novel indices, the expected energy not supplied cost (EENSC) and the expected travel time cost (ETTC). Both indices are stated as,

$$EENSC = C^{\mathrm{P}} \times EENS \tag{11}$$

$$ETTC = C^{T} \times \sum_{l_{pq}=1}^{\mathrm{N^T}} (TTI_{pq}^{\mathrm{ave}}) \tag{12}$$

where $\mathrm{C^P}$ is the energy not supplied cost for the PDS and $\mathrm{C^T}$ is the travel time cost for the UTS. To verify the impact of CLs on the coordinated PTS reliability, the scenario with no CLs is the base case. Additionally, the differential values, $\Delta EENSC$ and $\Delta ETTC$, are the corresponding reliability cost indices for the two systems as expressed in (13-14). Here, for the scenario with no CLs in the PTS, $EENS^{nCL}$, and $ETTI^{nCL}$ represent the indices for the PDS and UTS, respectively.

After converting both system indices into costs, the expected reliability cost for the PTS (ECPTS), shown in (15), is chosen as a novel reliability index to estimate the impact of CLs on improving the reliability of the coordinated PTS.

$$\Delta EENSC = EENSC^{nCL} - EENSC \tag{13}$$

$$\Delta ETTC = ETTC^{nCL} - ETTC \tag{14}$$

$$ECPTS = \Delta ETTC + \Delta EENSC \tag{15}$$

E. CHARGING STRATEGY IN A CL

Assume there are N^{CL} charging spots in one CL and every spot is associated with a charging pole where both conventional vehicles and EVs can park. The SOC_j of the j^{th} EV while parking and charging is expressed as [41],

$$SOC_j = SOC_j^{arr} + \frac{\eta P(t_j - t_j^{arr})}{C_j} \tag{16}$$

where C_j is the EV battery capacity and SOC_j is the real-time actual battery charge of the j^{th} EV in the CL. Each EV is charging as soon as it is parked in the CL at time t_j^{arr}. When the j^{th} EV has arrived at the CL, the initial SOC of the j^{th} EV is SOC_j^{arr}. SOC^{max} and SOC^{min} are the corresponding upper and lower SOC limits, respectively. If η is the charging efficiency, the EV charging constraints are stated as,

$$\begin{aligned} t_j &\in [t_j^{arr}, t_j^{dep}] \\ 0 &\le t_j - t_j^{arr} \le t_j^{dep} - t_j^{arr} \\ SOC_j^{\min} &\le SOC_j \le SOC_j^{\max} \end{aligned} \tag{17}$$

In this paper, SOC^{min} is the minimum charge state of one EV and is set at 20% of the battery capacity; SOC^{max} is set at 80%.

There are n^{CL} charging spots available at one specified time. The charging status of the j^{th} vehicle, S_j, is a binary variable at time t: $S_j = 1$ if the j^{th} vehicle is charging; $S_j = 0$ otherwise. Expressly, s_i is set to 0 if:

1) The EV is not in the CL;
2) The EV is charged to 80% of its battery capacity once parked in the CL. In this case, the EV may still be connected to the charging pole but will not be charged once wholly charged. For conventional vehicles, the charging status is 0 during the simulation.
3) The total charge is constrained due to PDS forced outages. For the j^{th} connected EV, the EV charging will be cut off if the PDS cannot supply the required energy.

The charging status is set to 1 if the EV is parked in the CL and its SOC_j is less than 80%. Besides, EVs depart from the CL for the next destination, where they will be fully charged again. By applying this strategy in SUMO, EVs will become charged to SOC^{max} while satisfying all constraints.

IV. CASE STUDY

In this work, SUMO is used to simulate traffic scenarios and obtain related data to calculate UTS reliability. SUMO simulates how a given traffic demand that consists of single vehicles moves through a given road. Here, SUMO is purely microscopic, in which each vehicle is modeled explicitly with its own route and moves individually through the network. Except for vehicles as the main simulation object, other components in the traffic system should also be modeled in SUMO as additional imported metadata. SUMO could be used to simulate traffic system microscopic behavior by considering almost all traffic system components. Other objects in the UTS, such as parking lots, intersections and traffic signals, are also configured and imported in SUMO. Both EVs and conventional vehicles are permitted to park in CLs.

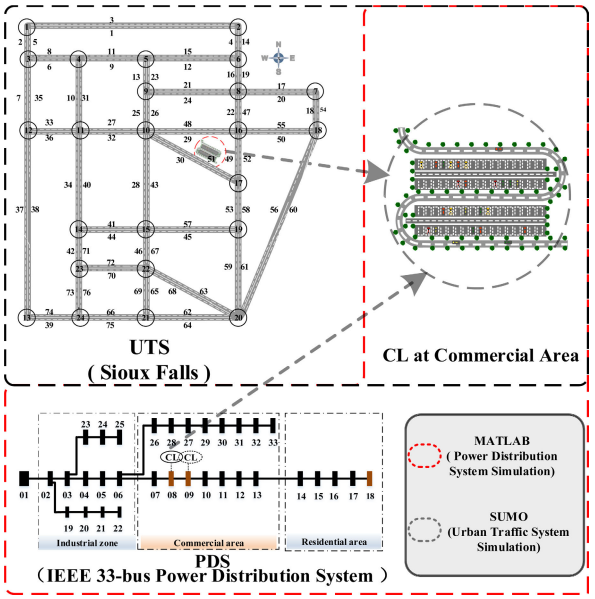

FIGURE 6. Case study topology for UTS and PDS.

In the case studies, the proposed framework assesses the impact of CL position on the coordinated PTS reliability. Different UTS edges located with CLs and different PDS buses connected to CLs are estimated. Various case studies are simulated, and detailed results are presented. UTS traffic flow is preconfigured in SUMO, and the load penetration profile [42] is used to build the PDS weekday load data. EV charging demand data in SUMO are updated in each SUMO simulation step. Here, the performance of the UTS and PDS without CLs is built and simulated first regarded as the base case for all reliability assessments. In the base scenario, the TTR indices for each edge are calculated. Then, CLs with charging spots are configured according to their capacity and locations and imported in SUMO for the other different scenarios. Here, we assume drivers choose to park in CLs in the afternoon commuting rush hours. A coordinated PTS coupled with a CL is shown in figure 6.

A. UTS TRAVEL TIME RELIABILITY

The Sioux Falls traffic network [43], chosen as the UTS model in this paper, has 24 nodes and 76 edges, which are illustrated in figure 6. For each UTS edge, there are two lanes with similar geometry. The speed limit in the UTS is set at 30 mph. Point-based sensors are located on each edge to capture continuous data to estimate the UTS performance. We also model certain factors as fixed, such as static traffic control strategies for traffic lights and the movement of individual vehicles.

System-level indices are evaluated by applying the process described in Section III. In this section, we calculate the PTI

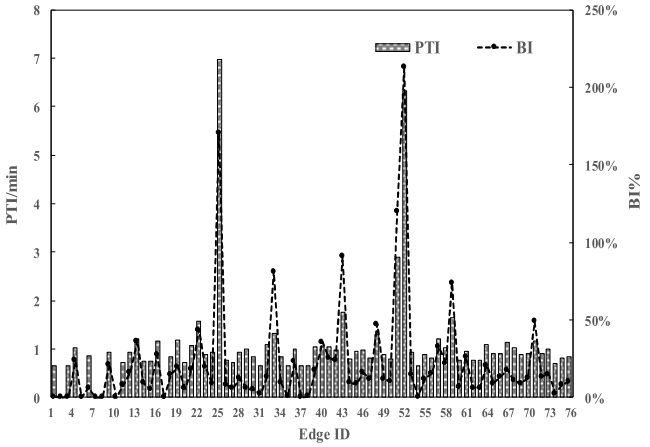

FIGURE 7. PTI and BI for each edge during afternoon commuting rush hours.

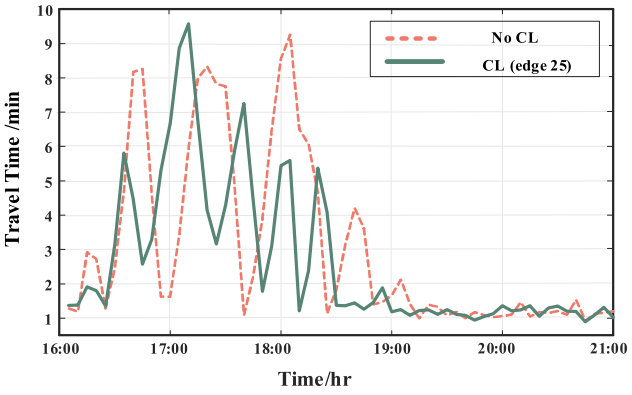

FIGURE 8. Travel time for edge 25 (no CL & CL along edge 25).

and BI for all UTS edges in the base scenario and show the results in figure 7. As the PTI is related to the $TT^{95\%}$ and TT^{free}, the BI is a function of $\overline{TT}$, so we choose the PTI and BI to be representatives to find the edge with the worst traffic condition. As shown in figure 7, edges with a higher PTI also have a higher BI. Edges 25, 43, 51, and 52 have the worst PTI and BI compared with the other edges, which are 6.98, 1.75, 2.89, and 6.33 and 170%, 91%, 120%, and 213%, respectively.

To estimate the impact of CL position on the coordinated PTS reliability, we consider CLs with the same capacity in different edges in SUMO. According to the results shown in figure 7, we built four scenarios where four CLs are located beside edges 25, 43, 51, and 52, respectively.

Case A: Some vehicles that pass edge **25** in their original route park at the CL belonging to edge **25**.

Case B: Some vehicles that pass edge **43** in their original route park at the CL belonging to edge **43**.

Case C: Some vehicles that pass edge **51** in their original route park at the CL belonging to edge **51**.

Case D: Some vehicles that pass edge **52** in their original route park at the CL belonging to edge **52**.

In each scenario, we estimated the impact of CL location by comparison with the results without the respective CL and present the results in Tables 1 and 2 and figures 8-11.

Compared with the base case, it can figure out the indices of UTS is changing with time. First, the edge-based indices show that a CL can reduce traffic congestion. As shown in Table 1, the variations and improvements of $TT^{95\%}$ and PTI are similar. It is because PTI is a linear function of the $TT^{95\%}$. Compared with scenarios that CL located on other edges, the CL located on edge 25 has a smaller impact on itself reliability improvement. The result can also be figured out from figure 8-11.

Meanwhile, CL along one edge can have a different impact on the network average performance compared with the impact on itself. For example, as tabulated in Table 1 and Table 2, even though the CL located on edge 52 makes the most improvement on itself edge-based reliability, the CL located at edge 52 makes less contribution to reducing the travel time reliability of the UTS. Conversely, the CL along edge 25 has the most impact on average reliability indices improvement, the contribution for edge-based reliability improvement is smallest. In detail, the decrease of average edge indices which CL located at edge 25 are 7.59%, 1.59%, 10.34%, and 25%, respectively.

TABLE 1. Comparison of edge-based indices.

Edge	Index	Without CL	With CL	Variation
25	$TT^{95\%}$/min	8.26	6.75	18.28%
	TTI /min	3.05	2.67	12.46%
	PTI /min	6.98	5.71	18.19%
	BI%	1.70	1.53	10.00%
43	$TT^{95\%}$ /min	4.57	3.02	33.92%
	TTI /min	2.39	2.18	8.79%
	PTI /min	1.75	1.16	33.71%
	BI%	0.91	0.38	58.24%
51	$TT^{95\%}$/min	6.64	4.32	34.94%
	TTI /min	3.01	2.80	6.98%
	PTI /min	2.89	1.88	34.95%
	BI%	1.20	0.54	55.00%
52	$TT^{95\%}$/min	7.43	3.98	46.43%
	TTI /min	2.37	1.99	16.03%
	PTI /min	6.33	3.3	47.87%
	BI%	2.13	0.99	53.52%

TABLE 2. Comparison of average edge indices.

Index	Edge	Without CL	With CL	Variation
$TT^{95\%}$/min	25	2.37	2.19	7.59%
	43	2.37	2.25	5.06%
	51	2.37	2.29	3.38%
	52	2.37	2.30	2.95%
TTI/min	25	1.89	1.86	1.59%
	43	1.89	1.86	1.59%
	51	1.89	1.88	0.53%
	52	1.89	1.89	0.00
PTI/min	25	1.16	1.04	10.34%
	43	1.16	1.08	6.90%
	51	1.16	1.12	3.45%
	52	1.16	1.10	5.17%
BI%	25	0.24	0.18	25.00%
	43	0.24	0.21	12.50%
	51	0.24	0.22	8.33%
	52	0.24	0.22	8.33%

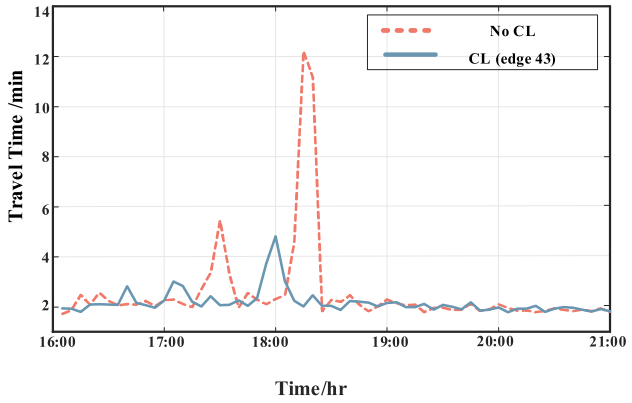

FIGURE 9. Travel time for edge 43 (no CL & CL along edge 43).

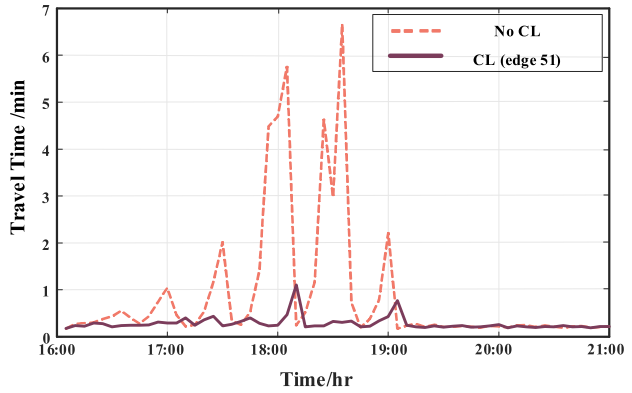

FIGURE 10. Travel time for edge 51 (no CL & CL along edge 51).

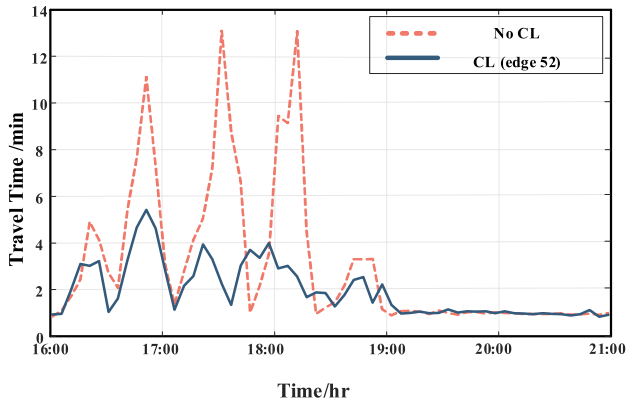

FIGURE 11. Travel time for edge 52 (no CL & CL along edge 52).

Therefore, compared with the base case, some social factors, such as the demand for cheaper electricity, can attract customers to stop at CLs and reduces the congestion on the road in the UTS, especially in the afternoon commuting rush hours.

B. PDS RELIABILITY ESTIMATION

Unlike conventional means of transportation, EVs can also be charged while parked at CLs. For this reason, when EVs choose to park at CLs, the UTS traffic conditions in the UTS could influence the charging time and energy required for

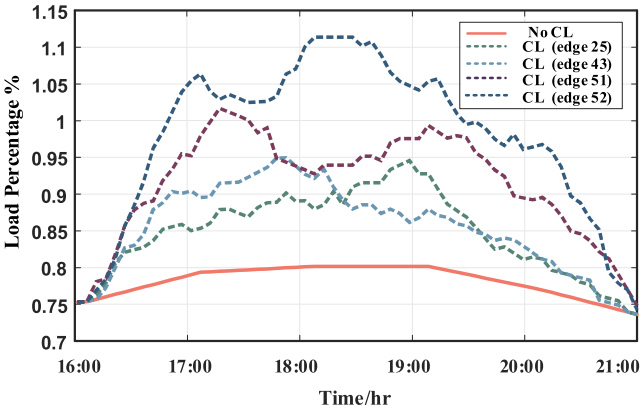

FIGURE 12. Bus 8 (Commercial CL) total load profiles.

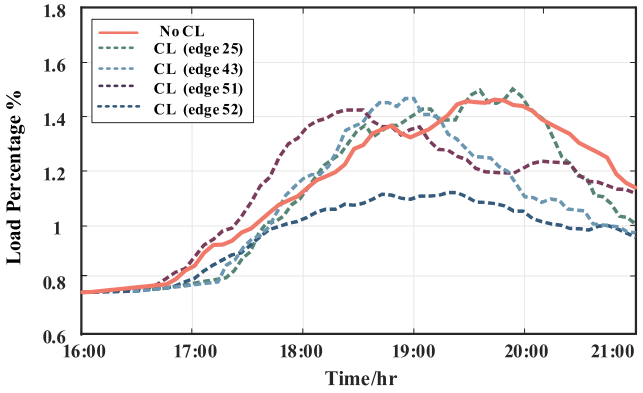

FIGURE 13. Bus 18 (Residential CL) total load profiles.

charging. Furthermore, choosing different electrical buses to supply energy to the same CL has different impacts on the PDS reliability.

In this section, we also discuss the PDS reliability considering a CL along edges 25, 43, 51, and 52, separately. The presence of no CLs in the UTS is also considered as the base case for the PDS reliability assessment. In order to focus on the impact of CL implementation on the PDS, the number of EVs is set as 35% of all parked vehicles in a CL. Additionally, the IEEE 33-bus PDS [44] is divided into three areas representing industrial, commercial, and residential areas. Buses 8 and 9 are chosen to supply charging energy for commercial CLs, and x bus 18 is connected with residential charging facilities.

In each scenario, the PDS reliability assessment is estimated by using the process presented in Section III. The Chevrolet Bolt [45], one type of EV, is chosen as the EV model built in SUMO in our simulation. Table 3 shows the parameters of this Chevrolet EV.

Cases A to D are the 4 scenarios that are used to analyze the impact of commercial area CLs on the PDS, and the results are presented in Table 4. The load profiles of buses 8 and 18 are illustrated in figures 12 and 13, respectively.

As shown in Table 4, the EENS values in scenarios with a CL are all less than the base case. It makes sense that the reliability can be improved more by putting a load on

TABLE 3. EV (Chevrolet Bolt) parameters.

EV parameters			
General Vehicle Data		**Electric Data**	
mass (kg)	1624	charging model	fast charging
maximum velocity	40.68 m/s	battery capacity	60 kWh
air drag coefficient	0.29	constant power intake	7.2 km
acceleration	3.8 m/s^2	charging efficiency	0.88
deceleration	4.5 m/s^2		
vehicle length	4.17 m		

TABLE 4. EENS for all cases.

	EENS (kWh/5min)			△EENS (kWh/5min)	
	Without CL	With CL			
		Bus 8	Bus 9	Bus 8	Bus 9
Case A	985.80	984.72	985.03	1.08	0.77
Case B	986.14	984.96	985.14	1.18	1
Case C	988.16	985.89	987.53	2.27	0.63
Case D	990.63	984.31	984.91	6.32	5.72

the bus closer to the power source instead of away from the power source. As TraCI4MATLAB extracts charging load information every 5 min and we assume the charging load is constant in each 5 min, we calculate the ENS in each 5 min and obtain the EENS. If we calculate the EENS for a longer duration, the amount of EENS would be significantly different.

As shown in figure 12, EVs parked at CLs caused a significant load increase on bus 8. Among the four scenarios, EVs charging at CL 52 presented the highest load increment, as edge 52 has the enormous traffic demand in the afternoon commuting rush hours. The residential charging load profile shows that the demand for home charging is less than the base case where EVs can only recharge at the residential bus. As illustrated in figure 13, the peak load of bus 18 in some scenarios is less than the base case. Meanwhiles, the decreasing time point of residential load is slightly shifted to the left as some EVs have charged on a commercial CL for a while.

Moreover, the residential charging load profiles might reflect the route traffic conditions as well. The significant increasing time of some residential bus profiles is a slightly shifted to the right because EV drivers charged while on the route. The result implies that shopping on the way back home might not be a bad choice. From the perspective of customer service, the social value of commercial CLs might need more attention.

C. COORDINATED PTS RELIABILITY ASSESSMENT

The framework presented in section II is used here to estimate the reliability of the coordinated PTS. Different cost values are used to weight the loads in different functional areas in the PDS[46]. For the UTS, the travel time cost is set to 6$/h for drivers in the afternoon commuting rush hours. The cost parameters for the two systems are listed below.

TABLE 5. Load and time unit costs for the PDS and UTS.

PDS	industrial	1.2	$/kW
	commercial	1	$/kW
	residential	0.0892	$/kW
UTS		6	$/hr

TABLE 6. Costs of all scenarios for the coordinated PTS.

CL	△ECOST (k$)(Bus 8)	△TTC (k$)	RCRTS (k$)
25	10.438	36.341	46.779
43	13.628	36.341	49.969
51	25.16	9.504	34.664
52	27.26	0	27.26

The scenario where a CL is located at edge 43 has the highest impact on the PTS reliability, reducing a total scenario cost of 49.969 k$. CLs located at different edges will have various impacts on the UTS and PDS. In essence, CL at edge 52 will save money for the PDS; however, the most economical UTS scenario is the CL at edge 43. It may be caused by different conditions on roads 52 and 43, even though the total number of EVs that will choose to stop at the CL is the same. It is because the number of conventional vehicles that choose to travel and park in each scenario is different. In other words, the driving behaviors of other vehicles (e.g., conventional vehicles) have a significant impact on the reliability of the coordinated system.

V. CONCLUSION

As a coupling component between the UTS and PDS, CL is an essential participant that influences the reliability of future smart cities constructed with the UTS and the PDS. This paper focuses on the reliability evaluation of the impact of CLs on the UTS and PDS. Considering the EV charging in a CL, the reliability of the coordinated system is evaluated and quantified using one unified index. SUMO realizes the UTS real-time simulation. The MCS method is used to obtain the state samples for branch outages in the PDS.

From the results of the comparison, it is observed that CL has a significant impact on the system-level reliability of UTS and PDS. What's more, the impact on the UTS and PDS are different. According to the coordinated PTS connection typology given in this paper, the influence that one specific CL has on the UTS is not the same as for the PDS. Therefore, it is crucial to calculate the reliability of the two systems together and an expertise unified index should be used for the coordinated PTS. Considering the interaction among various traffic factors, SUMO has been identified to be an excellent selection to analyze the time-varying UTS with congestion.

Consequently, we propose an integrated novel framework to evaluate the system-level reliability of coordinated PTS. Further, the TraCI in MATLAB successfully realizes the cooperation between the SUMO and MATLAB to analyze the time-varying indices under congestion. The reliability model and indices of a short-term coordinated UTS and PDS provide

the flexibility for the further reliability evaluation of a smart city.

REFERENCES

[1] *New Electric Vehicle Sales Market Share for 2016, 2017 and Forecast for 2018 (Full Year) for Selected Markets*. Accessed: Feb. 2019. [Online]. Available: https://evadoption.com/ev-market-share/
[2] M. H. Amini, J. Mohammadi, and S. Kar, "Distributed holistic framework for smart city infrastructures: Tale of interdependent electrified transportation network and power grid," *IEEE Access*, vol. 7, pp. 157535–157554, 2019.
[3] I. Pavić, T. Capuder, and I. Kuzle, "Value of flexible electric vehicles in providing spinning reserve services," *Appl. Energy*, vol. 157, pp. 60–74, Nov. 2015.
[4] Q. Zhou, M. Shahidehpour, M. Yan, X. Wu, A. Alabdulwahab, and A. Abusorrah, "Distributed secondary control for islanded microgrids with mobile emergency resources," *IEEE Trans. Power Syst.*, to be published.
[5] A. Mohamed, V. Salehi, T. Ma, and O. Mohammed, "Real-time energy management algorithm for plug-in hybrid electric vehicle charging parks involving sustainable energy," *IEEE Trans. Sustain. Energy*, vol. 5, no. 2, pp. 577–586, Apr. 2014.
[6] F. Li, H. Guo, Z. Jing, Z. Wang, and X. Wang, "Peak and valley regulation of distribution network with electric vehicles," *J. Eng.*, vol. 2019, no. 16, pp. 2488–2492, Mar. 2019.
[7] A. M. Bozorgi, M. Farasat, and A. Mahmoud, "A time and energy efficient routing algorithm for electric vehicles based on historical driving data," *IEEE Trans. Intell. Veh.*, vol. 2, no. 4, pp. 308–320, Dec. 2017.
[8] *National Travel Survey*, Dept. Transp., Stationery Office London, London, U.K., 2004.
[9] R. Chen, X. Qian, L. Miao, and S. V. Ukkusuri, "Optimal charging facility location and capacity for electric vehicles considering route choice and charging time equilibrium," *Comput. Oper. Res.*, vol. 113, Jan. 2020, Art. no. 104776.
[10] Q. Liu, J. Liu, W. Le, Z. Guo, and Z. He, "Data-driven intelligent location of public charging stations for electric vehicles," *J. Cleaner Prod.*, vol. 232, pp. 531–541, Sep. 2019.
[11] A. S. Nair, T. Hossen, M. Campion, and P. Ranganathan, "Optimal operation of residential EVs using DNN and clustering based energy forecast," in *Proc. North Amer. Power Symp. (NAPS)*, Sep. 2018, pp. 1–6.
[12] X. Liu and Z. Bie, "Optimal allocation planning for public EV charging station considering AC and DC integrated chargers," *Energy Procedia*, vol. 159, pp. 382–387, Feb. 2019.
[13] T. Zeng, S. Moura, and H. Zhang, "Solving overstay and stochasticity in PEV charging station planning with real data," *IEEE Trans. Ind. Informat.*, to be published.
[14] M. Rahmani-Andebili, "Robust operation of a reconfigurable electrical distribution system by optimal charging management of plug-in electric vehicles considering the technical, social, and geographical aspects," in *Planning Operation Plug-In Electric Vehicles*, M. Rahmani-Andebili, Ed. Cham, Switzerland: Springer, 2019, pp. 75–104.
[15] P. Salyani, M. Abapour, and K. Zare, "Stackelberg based optimal planning of DGs and electric vehicle parking lot by implementing demand response program," *Sustain. Cities Soc.*, vol. 51, Nov. 2019, Art. no. 101743.
[16] Y. Zhou, A. Ravey, and M.-C. Péra, "A survey on driving prediction techniques for predictive energy management of plug-in hybrid electric vehicles," *J. Power Sources*, vol. 412, pp. 480–495, Feb. 2019.
[17] M. Alizadeh, H.-T. Wai, M. Chowdhury, A. Goldsmith, A. Scaglione, and T. Javidi, "Optimal pricing to manage electric vehicles in coupled power and transportation networks," *IEEE Trans. Control Netw. Syst.*, vol. 4, no. 4, pp. 863–875, Dec. 2017.
[18] B. Canizes, J. Soares, A. Costa, T. Pinto, F. Lezama, P. Novais, and Z. Vale, "Electric vehicles' user charging behaviour simulator for a smart city," *Energies*, vol. 12, no. 8, p. 1470, Apr. 2019.
[19] M. H. Amini, M. P. Moghaddam, and O. Karabasoglu, "Simultaneous allocation of electric vehicles' parking lots and distributed renewable resources in smart power distribution networks," *Sustain. Cities Soc.*, vol. 28, pp. 332–342, Jan. 2017.
[20] A. Alturiman and M. Alsabaan, "Impact of two-way communication of traffic light signal-to-vehicle on the electric vehicle state of charge," *IEEE Access*, vol. 7, pp. 8570–8581, 2019.
[21] M. Amini and O. Karabasoglu, "Optimal operation of interdependent power systems and electrified transportation networks," *Energies*, vol. 11, no. 1, p. 196, Jan. 2018.
[22] R. Sabzehgar, M. A. Kazemi, M. Rasouli, and P. Fajri, "Cost optimization and reliability assessment of a microgrid with large-scale plug-in electric vehicles participating in demand response programs," *Int. J. Green Energy*, vol. 17, no. 2, pp. 127–136, Jan. 2020.
[23] S. Davidov and M. Pantoš, "Optimization model for charging infrastructure planning with electric power system reliability check," *Energy*, vol. 166, pp. 886–894, Jan. 2019.
[24] K. Hou, X. Xu, H. Jia, X. Yu, T. Jiang, K. Zhang, and B. Shu, "A reliability assessment approach for integrated transportation and electrical power systems incorporating electric vehicles," *IEEE Trans. Smart Grid*, vol. 9, no. 1, pp. 88–100, Jan. 2018.
[25] W. Wei, S. Mei, L. Wu, M. Shahidehpour, and Y. Fang, "Optimal traffic-power flow in urban electrified transportation networks," *IEEE Trans. Smart Grid*, vol. 8, no. 1, pp. 84–95, Jan. 2017.
[26] Q. Zhang, Y. Zhu, Z. Wang, Y. Su, and C. Li, "Reliability assessment of distribution network and electric vehicle considering quasi-dynamic traffic flow and vehicle-to-grid," *IEEE Access*, vol. 7, pp. 131201–131213, 2019.
[27] U. R. Prasanna, M. Srinivas, and L. Umanand, "Macroscopic model of city traffic using bond graph modelling," *Int. J. Eng. Syst. Model. Simul.*, vol. 1, nos. 2–3, p. 176, 2009.
[28] Z. Li, M. Shahidehpour, S. Bahramirad, and A. Khodaei, "Optimizing traffic signal settings in smart cities," *IEEE Trans. Smart Grid*, vol. 8, no. 5, pp. 2382–2393, Sep. 2017.
[29] P. A. Lopez, E. Wiessner, M. Behrisch, L. Bieker-Walz, J. Erdmann, Y.-P. Flotterod, R. Hilbrich, L. Lucken, J. Rummel, and P. Wagner, "Microscopic traffic simulation using SUMO," in *Proc. 21st Int. Conf. Intell. Transp. Syst. (ITSC)*, Nov. 2018, pp. 2575–2582.
[30] S. Krauß, "Microscopic modeling of traffic flow: Investigation of collision free vehicle dynamics," DLR—Deutsches Zentrumfür Luft- Raumfahrt e.V., Cologne, Germany, Tech. Rep. 98-08, 1998.
[31] J. Erdmann, "SUMO's lane-changing model," in *Modeling Mobility With Open Data* (Lecture Notes in Control and Information Sciences). Cham, Switzerland: Springer, 2015, pp. 105–123.
[32] A. F. Acosta, J. E. Espinosa, and J. Espinosa, "TraCI4Matlab: Enabling the integration of the SUMO road traffic simulator and MATLAB® through a software re-engineering process," in *Modeling Mobility With Open Data*. Cham, Switzerland: Springer, 2015, pp. 155–170.
[33] K. J. Nutt, "A comparison of techniques for assessing dispersal behaviour in gundis: Revealing dispersal patterns in the absence of observed dispersal behaviour," *Mol. Ecol.*, vol. 17, no. 15, pp. 3541–3556, Aug. 2008.
[34] U.S. Department of Transportation and Federal Highway Administration. (2006). *Travel Time Reliability: Making It There On Time, All The Time*. [Online]. Available: https://ops.fhwa.dot.gov/publications/tt_reliability/TTR_Report.htm#Whatmeasures
[35] W. Zhang, S. Guhathakurta, and E. B. Khalil, "The impact of private autonomous vehicles on vehicle ownership and unoccupied VMT generation," *Transp. Res. C, Emerg. Technol.*, vol. 90, pp. 156–165, May 2018.
[36] *Roadway Information and Traffic Monitoring System Program*. Accessed: Jul. 2019. [Online]. Available: https://www.state.nj.us/transportation/refdata/roadway/vmt.shtm
[37] *Simulation/Output/Lane-OR Edge-Based Traffic Measures*. Accessed: Jun. 2019. [Online]. Available: https://sumo.dlr.de/wiki/Simulation/Output/Lane-_or_Edge-based_Traf_c_Measures
[38] *Demand/Importing O/D Matrices*. Accessed: Jul. 2019. [Online]. Available: https://sumo.dlr.de/docs/Demand/Importing_O/D_Matrices.html
[39] R. Billinton and W. Li, *Reliability Assessment of Electric Power Systems Using Monte Carlo Methods*. Boston, MA, USA: Springer, 1994.
[40] J. Mello, M. Pereira, and A. Leite Da Silva, "Evaluation of reliability worth in composite systems based on pseudo-sequential Monte Carlo simulation," *IEEE Trans. Power Syst.*, vol. 9, no. 3, pp. 1318–1326, Aug. 1994.
[41] L. Yao, W. H. Lim, and T. S. Tsai, "A real-time charging scheme for demand response in electric vehicle parking station," *IEEE Trans. Smart Grid*, vol. 8, no. 1, pp. 52–62, Jan. 2017.
[42] C. Grigg, P. Wong, P. Albrecht, R. Allan, M. Bhavaraju, R. Billinton, Q. Chen, C. Fong, S. Haddad, S. Kuruganty, W. Li, R. Mukerji, D. Patton, N. Rau, D. Reppen, A. Schneider, M. Shahidehpour, and C. Singh, "The IEEE reliability test system-1996. A report prepared by the reliability test system task force of the application of probability methods subcommittee," *IEEE Trans. Power Syst.*, vol. 14, no. 3, pp. 1010–1020, Aug. 1999.
[43] M. Miralinaghi, Y. Lou, Y.-T. Hsu, R. Shabanpour, and Y. Shafahi, "Multiclass fuzzy user equilibrium with endogenous membership functions and risk-taking behaviors," *J. Adv. Transp.*, vol. 50, no. 8, pp. 1716–1734, Dec. 2016.

[44] M. E. Baran and F. F. Wu, "Network reconfiguration in distribution systems for loss reduction and load balancing," *IEEE Power Eng. Rev.*, vol. 9, no. 4, pp. 101–102, Apr. 1989.
[45] *Chevrolet Bolt*. Accessed: May 2019. [Online]. Available: https://en.wikipedia.org/wiki/Chevrolet_Bolt
[46] P. Wang and R. Billinton, "Reliability cost/worth assessment of distribution systems incorporating time-varying weather conditions and restoration resources," *IEEE Trans. Power Del.*, vol. 17, no. 1, pp. 260–265, Aug. 2002.

CHI ZHANG (Student Member, IEEE) received the B.S. degree from the School of Electrical Engineering, Chongqing University, China, in 2014, where she is currently pursuing the Ph.D. degree. She was a Visiting Scholar with the Robert W. Galvin Center for Electricity Innovation, Illinois Institute of Technology. Her research interests include reliability evaluation and optimization of coordinated transportation and power systems.

XIA ZHAO (Member, IEEE) received the Ph.D. degree in electrical engineering from Chongqing University, Chongqing, China, in 2009. She is currently an Associate Professor with the School of Electrical Engineering, Chongqing University. Her research interests include optimal dispatch, risk assessment of power systems, and integrated energy systems.

MOHAMMAD SHAHIDEHPOUR (Fellow, IEEE) received the Honorary Doctorate degree from the Polytechnic University of Bucharest, Bucharest, Romania. He is currently a University Distinguished Professor and the Director of the Robert W. Galvin Center for Electricity Innovation, Illinois Institute of Technology. Dr. Shahidehpour is a member of the U.S. National Academy of Engineering. He was a recipient of the 2019 IEEE PES Ramakumar Family Renewable Energy Excellence Award.

WENYUAN LI (Life Fellow, IEEE) is currently a Professor with Chongqing University, Chongqing, China. His research interests include power system planning, operation, optimization, and reliability assessment. He is a Fellow of the Canadian Academy of Engineering and the Engineering Institute of Canada, and a Foreign Member of the Chinese Academy of Engineering. He was a recipient of several IEEE PES awards, including the IEEE PES Roy Billinton Power System Reliability Award, in 2011, and the IEEE Canada Electric Power Medal, in 2014.

LILI WEN is currently an Engineer with the State Grid Chongqing Economic Research Institute, Chongqing, China. His research interest includes power system planning and analysis.

ZHIFANG YANG (Member, IEEE) received the Ph.D. degree in electrical engineering from Tsinghua University, in 2018. He is currently an Assistant Professor with Chongqing University. His research interests include power system analysis and the electricity market.